THE JOURNAL OF BIOLOGICAL CHEMISTRY
Vol. 277, No. 35, Issue of August 30, pp. 31722–31733, 2002

Printed in U.S.A.

A Novel Lipoarabinomannan from the Equine Pathogen *Rhodococcus equi*

STRUCTURE AND EFFECT ON MACROPHAGE CYTOKINE PRODUCTION*

Received for publication, March 28, 2002, and in revised form, May 31, 2002
Published, JBC Papers in Press, June 18, 2002, DOI 10.1074/jbc.M203008200

Natalie J. Garton‡§, Martine Gilleron§¶, Thérèse Brando¶, Han-Hong Dan‖, Steeve Giguère, Germain Puzo¶, John F. Prescott‖, and Iain C. Sutcliffe‡ ‡‡**

*From the ‡Institute of Pharmacy, Chemistry and Biomedical Sciences, the University of Sunderland, Sunderland SR2 3SD, United Kingdom, ¶Institut de Pharmacologie et de Biologie Structurale du CNRS, 205 Route de Narbonne, 31077 Toulouse Cedex 4, France, the ‖Department of Pathobiology, University of Guelph, Guelph, Ontario N1G 2W1, Canada, and **College of Veterinary Medicine, University of Florida, Gainesville, Florida 32610-0136*

***Rhodococcus equi* is a major cause of foal morbidity and mortality. We have investigated the presence of lipoglycan in this organism as closely related bacteria, notably *Mycobacterium tuberculosis*, produce lipoarabinomannans (LAM) that may play multiple roles as virulence determinants. The lipoglycan was structurally characterized by gas chromatography-mass spectrometry following permethylation, capillary electrophoresis after chemical degradation, and ^{1}H and ^{31}P and two-dimensional heteronuclear nuclear magnetic resonance studies. Key structural features of the lipoglycan are a linear α-1,6-mannan with side chains containing one 2-linked α-D-Man*p* residue. This polysaccharidic backbone is linked to a phosphatidylinositol mannosyl anchor. In contrast to mycobacterial LAM, there are no extensive arabinan domains but single terminal α-D-Ara*f* residue capping the 2-linked α-D-Man*p*. The lipoglycan binds concanavalin A and mannose-binding protein consistent with the presence of t-α-D-Man*p* residues. We studied the ability of the lipoglycans to induce cytokines from equine macrophages, in comparison to whole cells of *R. equi*. These data revealed patterns of cytokine mRNA induction that suggest that the lipoglycan is involved in much of the early macrophage cytokine response to *R. equi* infection. These studies identify a novel LAM variant that may contribute to the pathogenesis of disease caused by *R. equi*.**

Rhodococcus equi is a significant cause of disease in foals between the age of 1 and 5 months and is responsible for ~3% of global foal mortality (1). This organism has also emerged as an opportunistic human pathogen, notably of people with compromised immunity (2). *R. equi* is an intracellular pathogen of alveolar macrophages, and infection is characterized by bronchopneumonia. The bacterium is known to enter macrophages primarily (but not exclusively) via the complement receptor type 3 (Mac-1) following complement component C3 deposition (2, 3). Once within the macrophage the bacteria resist host-killing mechanisms and multiply, eventually killing the macrophage. Specific bacterial factors that facilitate entry of the organisms into the macrophages or that aid intra-macrophage persistence have yet to be identified.

R. equi is a member of the mycolata, a supra-generic taxon including the extensively studied facultative intracellular pathogen *Mycobacterium tuberculosis* (4). Members of the mycolata have a characteristic cell envelope architecture, dominated by lipids, notably the high molecular weight branched-chain mycolic acids. The cell envelope profoundly affects the properties of these bacteria, and its composition and organization have been a major focus of mycobacterial research (5, 6). Lipoarabinomannan (LAM)[1] is a complex mycobacterial cell envelope component that has been identified as a putative virulence factor of *M. tuberculosis* (7, 8). The structure of this macroamphiphile has been studied in detail and consists of a glycosylphosphatidylinositol anchor unit that bears a branched D-mannan and D-arabinan heteropolysaccharide. However, many elaborations of this core structure have been described, including variations in the pattern of the lipid anchor acylation, the presence of succinate residues, and capping motifs on the non-reducing termini of arabinan branches (7, 9–14). Some of these structural variations, notably the presence of particular capping motifs, may vary between the LAM of different mycobacterial species in a species-specific manner (7). To date LAM have been classified into ManLAM (15) and PILAM (16), according to their small mannooligosaccharide or phosphoinositide cap structures, respectively. The former were found in slow growing mycobacterial species (as *Mycobacterium bovis* BCG, *M. tuberculosis*), whereas the latter were found in fast growing mycobacterial species (as *Mycobacterium smegmatis*).

* This work was supported by The Horserace Betting Levy Board Grant vet/prj/652, by the Natural Sciences and Engineering Research Council of Canada, and by European Community Program TB Vaccine Cluster Contract QLK2-CT-1999-01093. The costs of publication of this article were defrayed in part by the payment of page charges. This article must therefore be hereby marked "*advertisement*" in accordance with 18 U.S.C. Section 1734 solely to indicate this fact.

§ Both authors contributed equally to the structural part of this work.
‡‡ To whom correspondence should be addressed. Tel.: 44 191 515 2995; Fax: 44 191 515 3747; E-mail: iain.sutcliffe@sunderland.ac.uk.

[1] The abbreviations used are: LAM, lipoarabinomannan; APTS, 1-aminopyrene-3,6,8-trisulfonate; Ara*f*, arabinofuranose; BHI, brain heart infusion; CE, capillary electrophoresis; DMEM, Dulbecco's modified Eagle's medium; FCS, fetal calf serum; GLC, gas liquid chromatography; G3PDH, glyceraldehyde-3-phosphate dehydrogenase; Gro, glycerol; HIC, hydrophobic interaction chromatography; HMBC, heteronuclear multiple bound correlation spectroscopy; HMQC, heteronuclear multiple quantum correlation spectroscopy; HOHAHA, homonuclear Hartmann-Hahn spectroscopy; IFN, interferon; IL, interleukin; Ins, inositol; LM, lipomannan; MALDI-TOF, matrix assisted laser desorption ionization-time of flight; Man*p* mannopyranose; ManLAM, LAM with mannosyl extensions; MBP, mannose-binding protein; PBS, phosphate-buffered saline; Ac_2PI, phosphatidylinositol; PILAM, LAM with phosphoinositide extensions; PIM, phosphatidylinositol mannosides; PIM_2, phosphatidylinositol dimannosides; Ac_3PIM_2 and Ac_4PIM_2, PIM_2 with 3 and 4 fatty acid appendages; ReqLAM, lipoglycan of *R. equi*; ROESY, rotating frame Overhauser effect spectroscopy; t, terminal; TNF-α, tumor necrosis factor α; LIF, laser-induced fluorescence; MS, mass spectrometry.

ManLAM has been shown to have many properties that potentially influence the pathogenicity of *M. tuberculosis*. In the early stages of infection, ManLAM may facilitate the adherence of bacteria to alveolar macrophages, particularly to mannose receptors (8, 17–19). It has been demonstrated that mycobacterial internalization via these receptors evades macrophage bactericidal mechanisms (20). LAM has also been reported to have powerful immunomodulatory properties, promoting distinctive patterns of macrophage cytokine induction that subsequently directs host immune responses (8, 21). Small differences in LAM structure can strongly influence these biological activities, demonstrating the value of detailed structural studies.

Lipoglycans apparently structurally related to LAM have been identified in representative organisms of other genera within the mycolata, including *Corynebacterium matruchotii* (22), *Dietzia maris* (23), *Gordonia rubropertincta* (24, 25), and *Rhodococcus rhodnii* (26). Although these lipoglycans display components typical of LAM, considerable variation in monosaccharide composition has been found. Thus, further detailed study of the lipoglycan components of these taxa is necessary. By analogy with mycobacterial ManLAM, we hypothesized that a lipoglycan may be involved in the pathogenic success of *R. equi*. This study describes the isolation, purification, and structural characterization of a *R. equi* lipoglycan. The potential role of this lipoglycan in *R. equi* virulence was assessed by comparing the early cytokine responses of equine macrophages to the lipoglycan and to infection with virulent *R. equi*.

EXPERIMENTAL PROCEDURES

Growth and Maintenance of Organisms—Three strains of *R. equi* were used in this study as follows: *R. equi* 103^+ (foal isolate) and *R. equi* 28^+ (pig isolate), which are clinical isolates containing plasmids associated with increased virulence (27); and the attenuated type strain *R. equi* ATCC 6939. Stock cultures were maintained on slopes of brain-heart infusion (BHI) agar (Oxoid, Unipath Ltd., Basingstoke, UK) at 4 °C. Cultures were maintained by routine subculture onto BHI agar and growth at 37 °C for 18 h. Broth cultures were grown in BHI broth incubated at 37 °C with shaking (200 rpm). for 18 h. Growth was then harvested, washed twice in PBS, and lyophilized.

Extraction of Lipoglycans—Lyophilized cells were delipidated with chloroform/methanol (1:1 v/v; 50 mg/ml) at ambient temperature for 18 h (28). The cells were then recovered by centrifugation (4000 rpm for 10 min) and washed twice with phosphate-buffered saline (PBS). Cells were then permeabilized with mutanolysin (50 units/ml) and lysozyme (25 mg/ml) according to the method of Assaf and Dick (29). An equal volume of phenol (90% w/v) was then added to the cell suspension in lysozyme buffer, and the mixture was incubated with shaking at 68 °C for 1 h to extract lipoglycans, which were subsequently recovered into the aqueous phase formed on refrigerated centrifugation as described previously (30).

Purification of the Lipoglycans—The crude aqueous extract was purified using a modification of the hydrophobic interaction chromatography (HIC) method (22, 31). Briefly, the crude extract was taken up into 6 ml of equilibration buffer (100 mM sodium acetate buffer, pH 4.5, containing 15% v/v *n*-propyl alcohol) and loaded onto a column (1.25 × 17 cm) of octyl-Sepharose CL-4B (Amersham Biosciences). The column was eluted with 40 ml of this buffer prior to gradient elution with a 120-ml gradient of 15–65% v/v *n*-propyl alcohol in 100 mM sodium acetate buffer, pH 4.5. Fractions were assayed for carbohydrate using the method of Fox and Robyt (32). HIC fractions were also monitored by SDS-PAGE. Samples (30 μl) of alternate fractions were prepared and electrophoresed. With consideration of SDS-PAGE analysis, carbohydrate-containing peak fractions were pooled, dialyzed extensively, and lyophilized. To remove a persistent protein contaminant from the lipoglycan, a 1 mg/ml aqueous solution of lipoglycan was treated with an equal volume of 90% phenol (w/v). The mixture was heated at 68 °C for 1 h and then separated into distinct aqueous and phenol phases by centrifugation (30 min, 4000 rpm, 4 °C). The upper aqueous phase was recovered and re-extracted with phenol. After further centrifugation, the aqueous phase was recovered and extensively dialyzed before being lyophilized and stored at −20 °C. Lipoglycan-containing fractions (PK3) were pooled, dialyzed, and lyophilized. Contaminants were removed by gel filtration. A sample (16 mg) was dissolved in 0.2 M NaCl, 0.25% sodium deoxycholate (w/v), 1 mM EDTA, and 10 mM Tris, pH 8, to a final concentration of 200 mg/ml, incubated 2 days at room temperature, and loaded on a gel permeation Bio-Gel P-100 column (52 × 3 cm) eluted with the same buffer at a flow rate of 5 ml/h.

Electrophoresis and Western Blotting Procedures—SDS-PAGE was performed as described by Laemmli (33) using 15% acrylamide resolving gels. The lipoglycan bands were characterized by silver staining with polysaccharide-specific periodic acid oxidation according to Tsai and Frasch (34). Western blotting and lectin blotting using concanavalin A were performed as described previously (23).

Analysis of Lipoglycan Carbohydrate and Fatty Acid Composition—Lipoglycan samples (1 mg) were acid-hydrolyzed with 2 M trifluoroacetic acid (250 μl) at 110 °C for 2 h in a 8.5 ml of polytetrafluoroethylene screw-capped tube. The hydrolysates were then neutralized *in vacuo* over sodium hydroxide pellets, and the dried residue was taken up in distilled water (250 μl) and then lyophilized. The monosaccharides were derivatized as alditol acetates and analyzed by GLC as described previously (23). Fatty acid composition of the lipoglycan samples (1 mg) was analyzed by GLC of the acid hydrolysate following derivatization to form fatty acid methyl esters as described previously (23). An Immunopure® recombinant mannose-binding protein (MBP) column (Pierce and Warriner Ltd., Chester, UK) was used to demonstrate interaction of lipoglycan with MBP as described previously (23).

Permethylation Analysis of Lipoglycan Samples—Lipoglycan (2 mg) from *R. equi* strains 103^+ and 28^+ was deacylated according to the method of Beachey *et al.* (35). The deacylated lipoglycans were permethylated according to the method of Dell *et al.* (36). The permethylated samples were cleaned using a C_{18} Sep-Pak Cartridge (Waters Associates). Each sample was taken up into chloroform/water (1:1 v/v, 1 ml). The cartridge was conditioned by sequential washing with distilled water (5 ml), acetonitrile (5 ml MeCN) and distilled water (10 ml). The sample was then loaded onto the cartridge and distilled water (5 ml) and 2 ml each of 15, 35, 50, and 75% aqueous MeCN and MeCN (2 ml) were used to elute the sample. Fractions collected at each step were assayed for carbohydrate as described previously (23) and by TLC in $MeCN/H_2O$ (85:15, v/v), visualizing with α-naphthol. Fractions that were found to contain carbohydrate were pooled and evaporated under nitrogen.

The permethylated samples were hydrolyzed with 2 M trifluoroacetic acid at 110 °C for 2 h as above. The methylated monosaccharides were then reduced with sodium borodeuteride and acetylated according to the method of Saddler *et al.* (37). Gas chromatography-mass spectrometry analysis of the samples was performed on a Carlo-Erba 8060 MS gas chromatograph connected to a Micromass Trio 2000 mass spectrometer. Samples were injected with a split injector (split rate of 50:1). The injection port temperature was 250 °C and the transfer line 250 °C. The column was a 30 m × 0.32 mm internal diameter BPX-5 fused silica column with helium (50 kPa) as the carrier gas. The oven was programmed to hold 140 °C for 1 min followed by a 10 °C/min rise to 280 °C and a 10-min hold. The mass spectrometer operated in electron ionization mode (70 eV) and was set to scan from 20 to 650 atomic mass units.

MALDI-TOF Analysis—Analysis by matrix-assisted laser desorption ionization-time of flight mass spectrometry (MALDI-TOF MS) was carried out on a Voyager DE-STR (Perspective Biosystems, Framingham, MA) using linear mode detection. All samples were irradiated with UV light (337 nm) from an N_2 laser and were analyzed with the instrument operating at 20 kV in the negative ion mode. The matrix used was 2,5-dihydroxybenzoic acid.

Acetolysis Procedure—10 μg of samples were treated with 15 μl of acetic anhydride/acetic acid/sulfuric acid (10:10:1, v/v/v) mixture for 3 h at 40 °C. The reaction was quenched by addition of 40 μl of water. Acetolysis products were extracted twice with 40 μl of chloroform and, after drying, were deacetylated with 20 μl of a methanol, 20% aqueous ammonia solution (1:1 v/v) at 37 °C for 18 h. The reagents were removed under a stream of nitrogen. The samples were then submitted to APTS tagging (see below).

APTS Derivatization—Dried hydrolysis (complete hydrolysis, 2 M trifluoroacetic acid at 110 °C for 2 h; mild hydrolysis, 0.1 M HCl at 110 °C for 30 min) or acetolysis (38) products were mixed with 0.4 μl of 0.2 M 1-aminopyrene-3,6,8-trisulfonate (APTS) (Interchim, Montluçon, France) in 15% (v/v) acetic acid and 0.4 μl of a 1 M sodium cyanoborohydride solution dissolved in tetrahydrofuran (39). The reaction was performed for 90 min at 55 °C and was quenched by addition of 20 μl of water. Dilutions of 1–5 μl of the APTS derivatives were prepared in 20 μl of total water before analysis by capillary electrophoresis (CE).

Capillary Electrophoresis—The electropherograms were acquired and stored on a Dell XPS P60 computer using the System Gold software

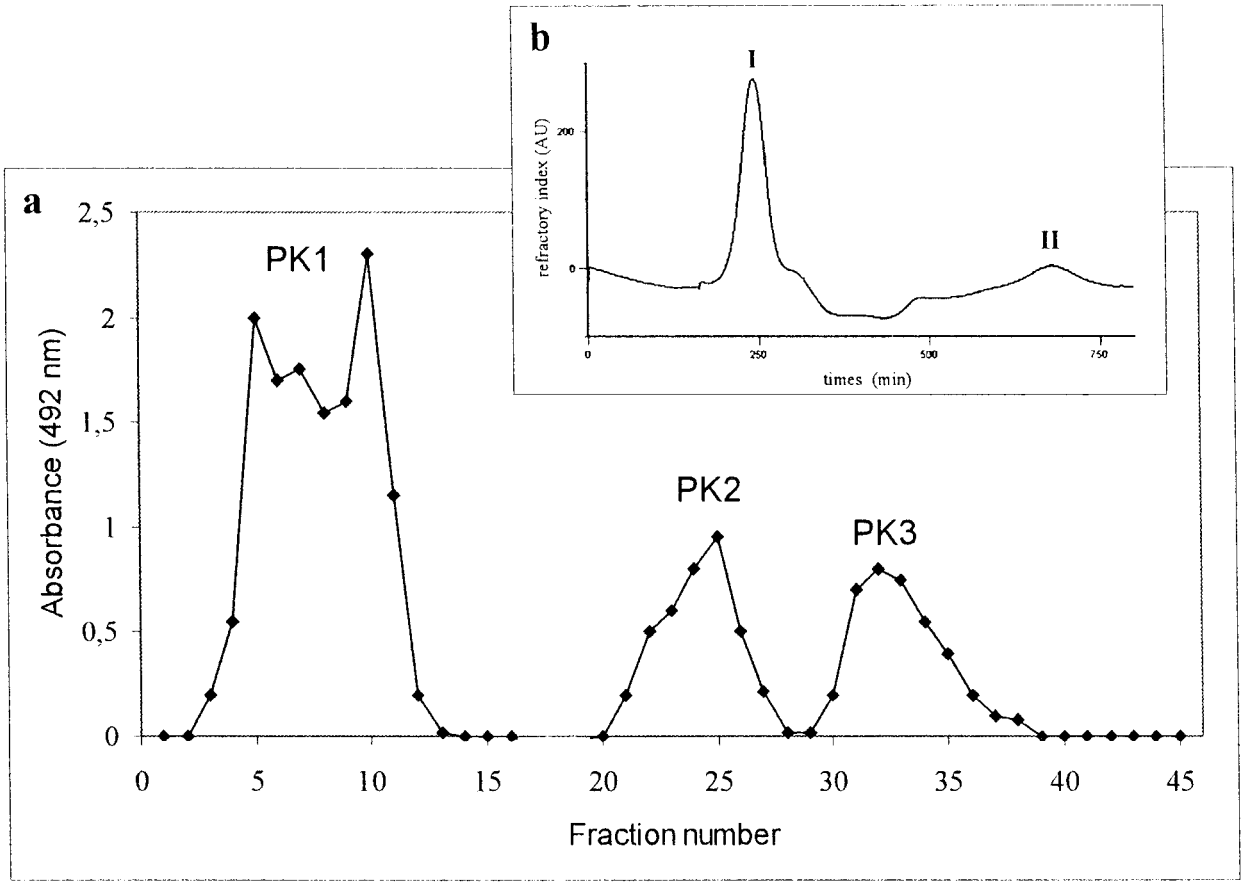

FIG. 1. **Purification of the lipoglycan fraction from *R. equi* 28$^+$.** *a,* crude phenol extract was loaded to the HIC column and washed to fraction 10 to remove hydrophilic contaminant material (*PK1*). Gradient elution with increasing concentrations of propanol (15–65% v/v; fractions 10–39) was used to recover two peaks of interest (*PK2* and *PK3*). Fractions 40–47 were eluted with 65% v/v propanol. Fractions (4.2 ml) were monitored by assay for carbohydrate (♦). *b,* lipoglycan-containing fractions (*PK3*) were pooled, dialyzed, lyophilized, and loaded on a Bio-Gel P-100 gel permeation column eluted with a deoxycholate-containing Tris buffer. Fraction I contained ReqLAM, and fraction II contained a contaminant.

package (Beckman Instruments). APTS derivatives were loaded by applying 0.5 pounds/square inch (3.45 kPa) vacuum for 5 s (6.5 nl injected). Separations were performed using an uncoated fused-silica capillary column (Sigma) of 50-μm internal diameter with 40-cm effective length (47 cm total length). Analyses were usually performed on a P/ACE capillary electrophoresis system (Beckman Instruments) with the cathode on the injection side and the anode on the detection side (reverse polarity) (Fig. 3, *a, c,* and *d*). They were carried out at a temperature of 25 °C with an applied voltage of −20 kV and using 1% acetic acid (w/v), 30 mM triethylamine in water, pH 3.5, as running electrolyte. For Fig. 3*b*, the electropherogram was recorded in normal mode, at a temperature of 25 °C with an applied voltage of +25 kV and borate buffer (20 mM, pH 9.2) as running electrolyte.

Detection system consisted in a Beckman laser-induced fluorescence (LIF) equipped with a 4-milliwatt argon-ion laser with the excitation wavelength of 488 nm and emission wavelength filter of 520 nm.

NMR Spectroscopy—Prior to NMR spectroscopic analysis, fractions were exchanged in D_2O (99.9% purity, Eurisotop, Saint Aubin, France) at room temperature with intermediate freeze-drying, and then dissolved in 400 μl of D_2O or Me_2SO-d_6 (99.8% purity, Eurisotop, Saint Aubin, France). ReqLAM from strain 28$^+$ (15 mg) and strain 103$^+$ (3 mg) was analyzed in a 200 × 5-mm 535-PP NMR tubes at 313 K on a Bruker DMX-500 500 MHz NMR spectrometer equipped with a double resonance (^{1}H/X)-BBi z-gradient probe head. Data were processed on a Bruker-X32 work station using the xwinnmr program. Proton and carbon chemical shifts are expressed in ppm downfield from internal acetone (δ_H/TMS 2.225 and δ_C/TMS 34.00). The one-dimensional phosphorus (^{31}P) spectra were measured at 202.46 MHz and phosphoric acid (85%) was used as the external standard (δ_P 0.0). All two-dimensional NMR data sets were recorded without sample spinning, and data were acquired in the phase-sensitive mode using the time-proportional phase increment method (40). Four two-dimensional Homonuclear Hartmann-Hahn (HOHAHA) spectra were recorded using MLEV-17 mixing sequences of 9, 43, 82, and 113 ms (41). The ^{1}H-^{13}C and ^{1}H-^{31}P single-bond correlation spectra (HMQC) were obtained using Bax's pulse sequence (42). The GARP sequence (43) at the carbon or phosphorus frequency was used as a composite pulse decoupling during acquisition. The pulse sequence used for ^{1}H-detected heteronuclear relayed spectra (HMQC-HOHAHA) was that of Lerner and Bax (44) and for HMBC was that of Bax and Summers (45).

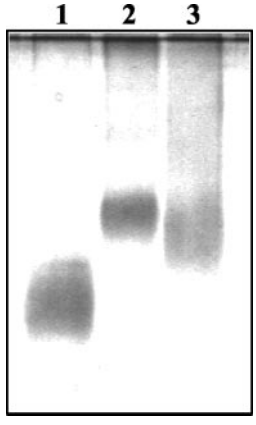

FIG. 2. **SDS-PAGE analysis of ReqLAM and related *M. bovis* BCG lipoglycans.** *Lane 1*, LM from *M. bovis* BCG; *lane 2*, ManLAM from *M. bovis* BCG; *lane 3*, PK3 fraction (ReqLAM) from *R. equi* strain 28$^+$. The gel was stained with a silver stain containing periodic acid.

Macrophage Culture—Peripheral blood macrophages were isolated from a healthy adult horse using Percoll (Sigma) and resuspended at 5 × 10^6 cells/ml in Dulbecco's modified Eagle's medium (DMEM; Invitrogen) with 10% fetal calf serum (FCS) supplemented with penicillin

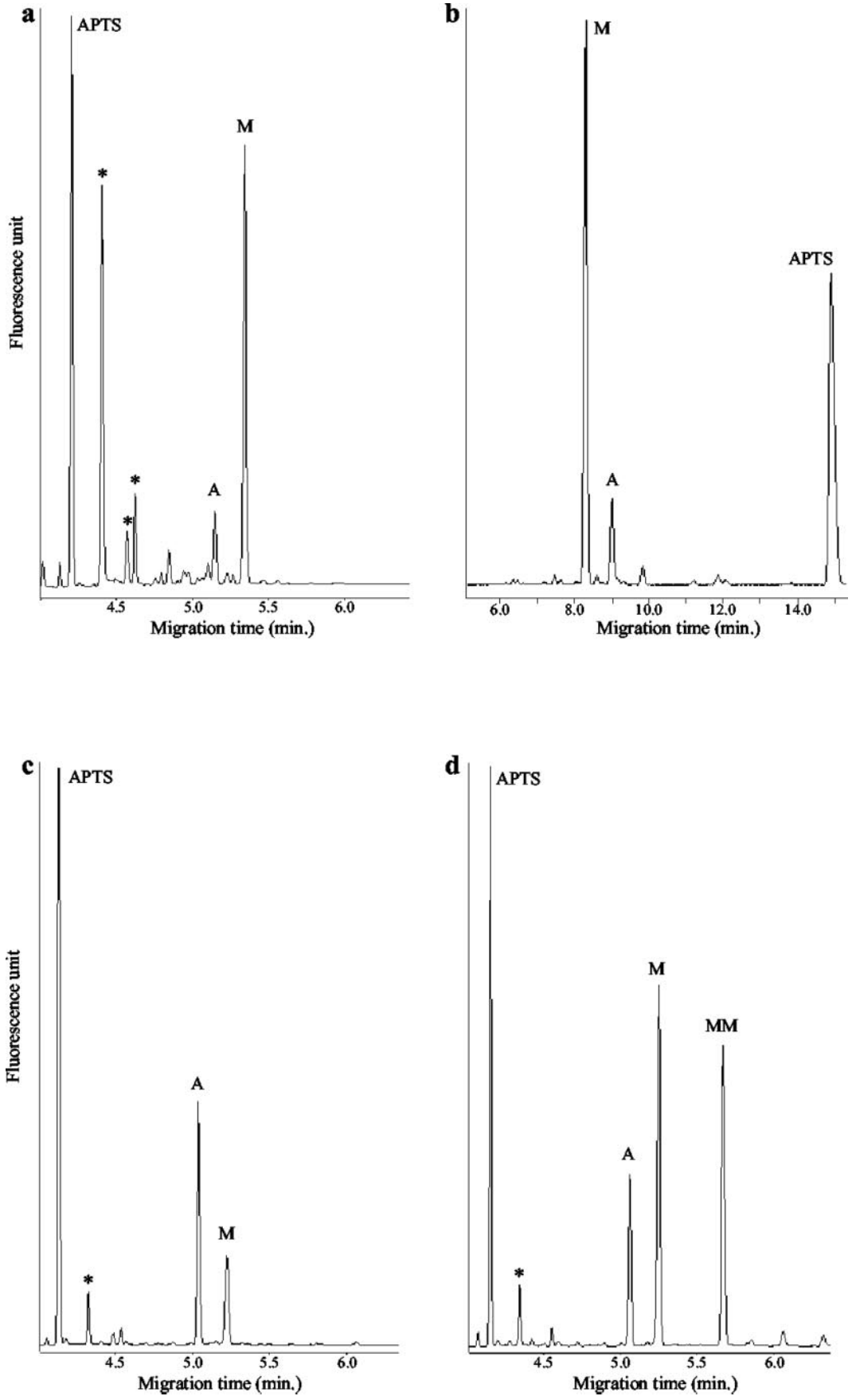

FIG. 3. **CE-LIF electropherograms of monosaccharide and oligosaccharide APTS derivatives resulting from total (*a* and *b*) or partial acid hydrolysis (*c*) and acetolysis of ReqLAM from strain 28$^+$ (*d*).** CE-LIF electropherograms of *a, c,* and *d* were carried out with an applied voltage of −20 kV and using acetic acid 1% (w/v), triethylamine 30 mM in water (pH 3.5) as running electrolyte. CE-LIF electropherogram of *b* was recorded in normal mode, with an applied voltage of +25 kV and borate buffer 20 mM (pH 9.2) as running electrolyte. *A*, Ara-APTS; *M*, Man-APTS; *MM*, Man$p\alpha$1→2Man-APTS. *Peaks* labeled with asterisks arise from the APTS reagent.

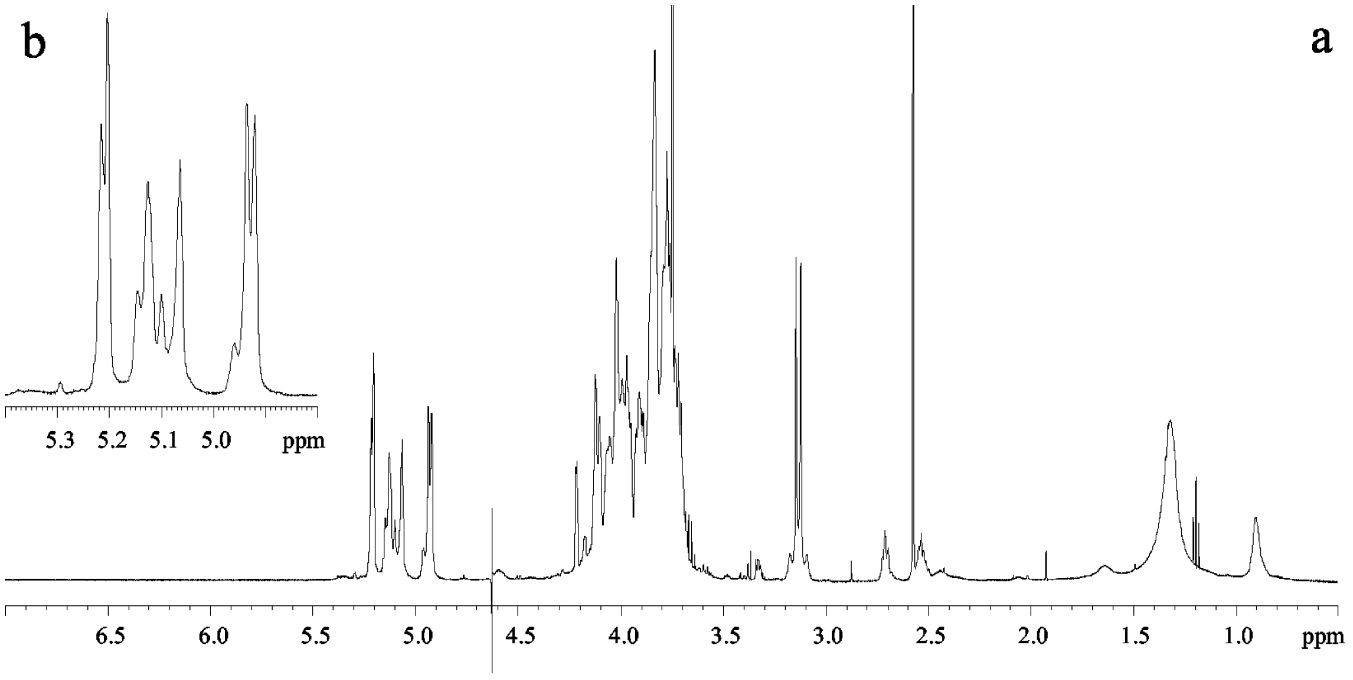

FIG. 4. **Expanded regions of the one-dimensional ^{1}H spectra (δ ^{1}H, 0.5–7.0) (*a*) and anomeric zone (δ ^{1}H, 4.8–5.4) (*b*) of the ReqLAM strain 28$^+$ in D_2O at 313 K.** The scan number was 128.

(100 μg/ml), streptomycin (80 μg/ml), and gentamicin (20 μg/ml). 1 ml of the suspension was placed in each well of a 24-well tissue culture plate, with 10 wells used for each treatment. Following overnight (18 h) incubation at 37 °C in a humidified atmosphere containing 5% CO_2, nonadherent cells were removed by washing the plate with warm DMEM/FCS with or without antibiotics for *R. equi* and lipoglycan treatments, respectively. Following 4–6 h of culturing, 2.5×10^6 cells remained in each well and were used for either bacterial infection or lipoglycan stimulation.

Bacterial Infection and Lipoglycan Stimulation—Initial studies were done to optimize lipoglycan concentration. Infection of horse macrophages with *R. equi* was carried out as described by Giguère and Prescott (46). A multiplicity ratio of 5 bacteria per macrophage was used. After 40 min of incubation to allow phagocytosis, the macrophages were washed three times and then incubated in DMEM/FCS with antibiotics in order to kill extracellular bacteria and to prevent further extracellular bacterial growth and reinfection of macrophages. For the time course study of lipoglycan stimulation, 10 μl of lipoglycan in phosphate-buffered saline, pH 7.2 (PBS), with 200 μg/ml polymyxin were added to each well to yield a final lipoglycan concentration of 5 μg/ml. Macrophages were harvested for RNA extraction at 0.7, 4, 8, 12, and 24 h following lipoglycan stimulation or exposure to *R. equi* for infection. Thus, the first time point for the *R. equi*-infected macrophages represents the time point at which infection was stopped by replacement with DMEM/FCS medium containing antibiotics. Untreated macrophages cultured under the same conditions were used as controls.

Quantitation of Cytokine mRNA Expression by Real Time PCR—Macrophages harvested at the times described above were centrifuged at $400 \times g$ for 5 min and washed with warm PBS, and total RNA was extracted using Qiagen RNeasy Mini Kit (Qiagen Inc., CA). All RNA samples were treated with amplification grade DNase I (Invitrogen) to remove any traces of genomic DNA contamination. 1 μg of total RNA was used for cDNA synthesis in a volume of 25 μl using the Thermoscript RT-PCR System kit (Invitrogen). After cDNA synthesis by reverse transcription, the reaction was diluted to 80 μl. Gene-specific primers and internal oligonucleotide probes for IL-1β, IL-6, IL-8, IL-10, IL-12p40, IL-18, TNF-α, and IFN-γ and glyceraldehyde-3-phosphate dehydrogenase (G3PDH) were selected based on equine cDNA sequences (Table III) using the Primer Express Software (Applied Biosystems, Foster City, CA). The internal probes were labeled at the 5′ end with the reporter dye 6-carboxyfluorescein, and at the 3′ end with the quencher dye 6-carboxytetramethylrhodamine. Amplification of 2 μl of cDNA was performed in a 25-μl PCR containing 900 nM of each primer, 250 nM of Taqman probe, and 12 μl of TaqMan Universal PCR Mastermix (Applied Biosystems). Amplification and detection were performed using the ABI Prism 7700 Sequence Detection System (Applied Biosystems) with initial incubation steps at 50 °C for 2 min and 95 °C for 10 min followed by 40 cycles of 95 °C for 15 s and 60 °C for 1 min. Each sample was assayed in triplicate, and the mean value was used for comparison. Samples without cDNA were included in the amplification reactions to determine background fluorescence and check for contamination. cDNA from 24-h concanavalin A-stimulated equine blood mononuclear cells was used as positive control. To account for variation in the amount and quality of starting material, all the results were normalized to G3PDH expression. Relative quantitation between samples was achieved by the comparative threshold cycles method and is reported as the *n*-fold difference relative to cytokine mRNA expression in unstimulated macrophages (47).

RESULTS

Purification of the Lipoglycan Fraction of R. equi

In order to minimize contamination with extractable lipids (particularly phosphatidylinositol dimannoside (PIM_2)) and to maximize yields, *R. equi* cells were delipidated and permeabilized prior to extraction with hot water/phenol (28, 48). The carbohydrate profile for the HIC purification of a crude hot water/phenol extract of *R. equi* 28$^+$ is shown in Fig. 1*a*. Similar results, with a reduced proportion of PK2, were obtained for the purification of extracts of *R. equi* 103$^+$ and ATCC 6939.

Initial elution of the column with equilibration buffer removed hydrophilic contaminant material that includes nucleic acids, polysaccharides, and proteins (*PK1,* Fig. 1*a*). Two carbohydrate-containing peaks eluted within the propanol gradient (*PK2* and *PK3*, Fig. 1*a*). Each fraction was analyzed by SDS-PAGE and modified silver staining which revealed PK3 to contain lipoglycan (ReqLAM). However, the final few fractions were contaminated with a low molecular weight mannose-containing lipid thought to be phosphatidylinositol mannosides (PIM) larger than PIM_2. Moreover, the fractions that composed PK2 were not revealed using this staining method and were subsequently shown to contain a very high molecular weight polysaccharide, the composition of which varied between strains, and no fatty acids. Consequently PK2 was thought to derive from capsular polysaccharide and as such was not studied further. Lipoglycan-containing fractions (PK3) were pooled, excluding those containing the low molecular weight contami-

TABLE I
Proton and carbon chemical shifts of strain 28$^+$ ReqLAM
Chemical shifts were measured at 313 K in D_2O and are referenced relative to internal acetone at δ_H 2.225 and δ_c 34.00.

System	Attribution	1	2	3	4	5	6
I	2-*O*-Linked α-Man*p*	104.2 5.21	80.4 4.12	73.4 3.91	69.9 3.75	76.3 3.78	64.2
II	t-α-Ara*f*	112.3 5.20	84.2 4.21	79.6 3.96	86.7 4.12	64.2 3.73/3.84	ND[a]
III	2,6-*O*-Linked α-Man*p*	101.3 5.15	81.7 4.05	 4.07	ND	ND	ND
IV	2,6-*O*-Linked α-Man*p*	101.3 5.12	81.7 4.06	73.6 3.98	69.7 3.83	74.1 3.83	69.9 3.73/3.83
V	4-*O*-Linked α-Man*p*	101.3 5.10	73.2 4.07	 3.96	ND	ND	ND
VI	t-α-Man*p*	105.2 5.06	73.1 4.10	74.1 3.83	69.9 3.71	76.3 3.77	64.0 3.70/3.90
VII	6-*O*-Linked α-Man*p*	102.4 4.96	 4.15	 4.05	ND	ND	68.7
VIII	6-*O*-Linked α-Man*p*	102.6 4.93	73.1 4.02	74.1 3.84	69.9 3.78	76.3 3.72	68.7 3.77/3.99
IX	6-*O*-Linked α-Man*p*	102.6 4.92	73.1 4.02	 3.85	 3.76	 ND	68.7

[a] ND, not determined.

nant. Following dialysis and lyophilization, HIC purified lipoglycan typically represented 0.4% of the dry cell weight extracted.

Subsequently, NMR studies revealed that PK3 was still contaminated by small mannose-containing molecules. The PK3 lipoglycan was further purified by gel filtration in presence of sodium deoxycholate buffer. Gel filtration chromatographic profile shows two peaks, I and II (Fig. 1*b*). Peak I was tentatively assigned to ReqLAM, based on its electrophoretic mobility on SDS-PAGE (Fig. 2). However, ReqLAM shows an electrophoretic behavior slightly different from those of *M. tuberculosis* and BCG ManLAM, in agreement with MALDI-TOF MS spectrum showing a broad peak centered at *m/z* 8000 (data not shown) indicating a molecular mass for the most abundant ReqLAM molecular species of 8 kDa. A molecular mass around 17 kDa was established for the BCG ManLAM (15, 38).

Structural Characterization of R. equi LAM

ReqLAM Polysaccharidic Backbone—The ReqLAM (strain 28$^+$) was first hydrolyzed (2 M trifluoroacetic acid for 2 h at 110 °C), and the resulting monosaccharides were derivatized with APTS and analyzed by CE (12). The electropherograms (Fig. 3, *a* and *b*) are dominated by one peak assigned to Man-APTS and a peak of lower intensity attributed to Ara-APTS in both running electrolytes used. From peak integration, the relative composition of the ReqLAM polysaccharide backbone was 86% Man*p* and 14% Ara*f*. Glycerol and inositol, components of a putative phosphatidylinositol anchor, were also detected by GC analysis. These data suggested that the *R. equi* lipoglycan may represent an unusual variant on the LAM archetype (ReqLAM).

Western blotting of the lipoglycan preparations with polyclonal anti-LAM antibody (raised against ManLAM from *M. tuberculosis*, strain H37Rv) demonstrated a weak positive cross-reaction only with material from *R. equi* 103$^+$ (results not shown). This was further indication that the lipoglycan from *R. equi* represents a structural variant of the mycobacterial LAM.

In order to investigate the glycosidic linkages present in the ReqLAM, the sample was deacylated, permethylated, hydrolyzed, and derivatized as alditol acetates. The various methylated alditol acetates were routinely identified by gas chromatography-mass spectrometry as terminal (t-), 2-, 2,6-, and 6-*O*-linked mannopyranose residues in 13, 12, 27, and 32% respective abundance with traces of 4-*O*-linked mannose. The majority of the arabinose present (11%), determined as being in the furanose form, was detected as terminal residues. From these data and by analogy to the BCG and *M. tuberculosis* ManLAM structure, a backbone of 6-*O*-linked Man*p* can be tentatively advanced. In addition, the presence of 2-*O*-linked Man*p* suggested that the branches may contain 2-*O*-linked Man*p* residues. The t-Man*p* and t-Ara*f* cap the 2-*O*-linked Man*p* or may be directly linked to the C-2 of linear 6-*O*-linked Man*p*. The presence of t-Man*p* residues was confirmed by lectin blotting of lipoglycan material using concanavalin A (not shown).

The absence of 5-*O*-linked Ara*f* and consequently of mannose caps which typify the BCG and *M. tuberculosis* ManLAM was supported by the following experiments. ReqLAM was submitted to mild acidic hydrolysis (0.1 M HCl for 30 min at 110 °C) followed by APTS derivatization and CE analysis (48). Mild hydrolysis leads to selective cleavage of Ara*f* links and consequently to the release of mannose caps with 1 Ara unit at the reducing end (12, 14, 38). The electropherogram (Fig. 3*c*) showed mainly two peaks assigned to Ara-APTS and Man-APTS supporting, as expected, the absence of (t-Man*p*→Ara*f*) sequence.

We then investigated whether t-Man*p* and t-Ara*f* cap the 2-*O*-linked Man*p* or are directly linked to the C-2 of linear 6-*O*-linked Man*p*. ReqLAM was submitted to acetolysis, which allows preferential cleavage of 6-*O*-linked hexopyranose and the Ara*f* linkages (38), followed by deacetylation, APTS derivatization, and CE analysis. Three peaks of interest (Fig. 3*d*) were observed assigned to Ara-APTS, Man-APTS, and Man*p*α1→2Man-APTS derivatives in the relative abundance of 20, 45, and 35%. This result indicated the existence of side chains composed of a single Man*p* capped selectively by t-Ara*f* and not-by t-Man*p*. This implied that t-Man*p* is linked directly to the 6-*O*-linked backbone. Moreover, a percentage of branch-

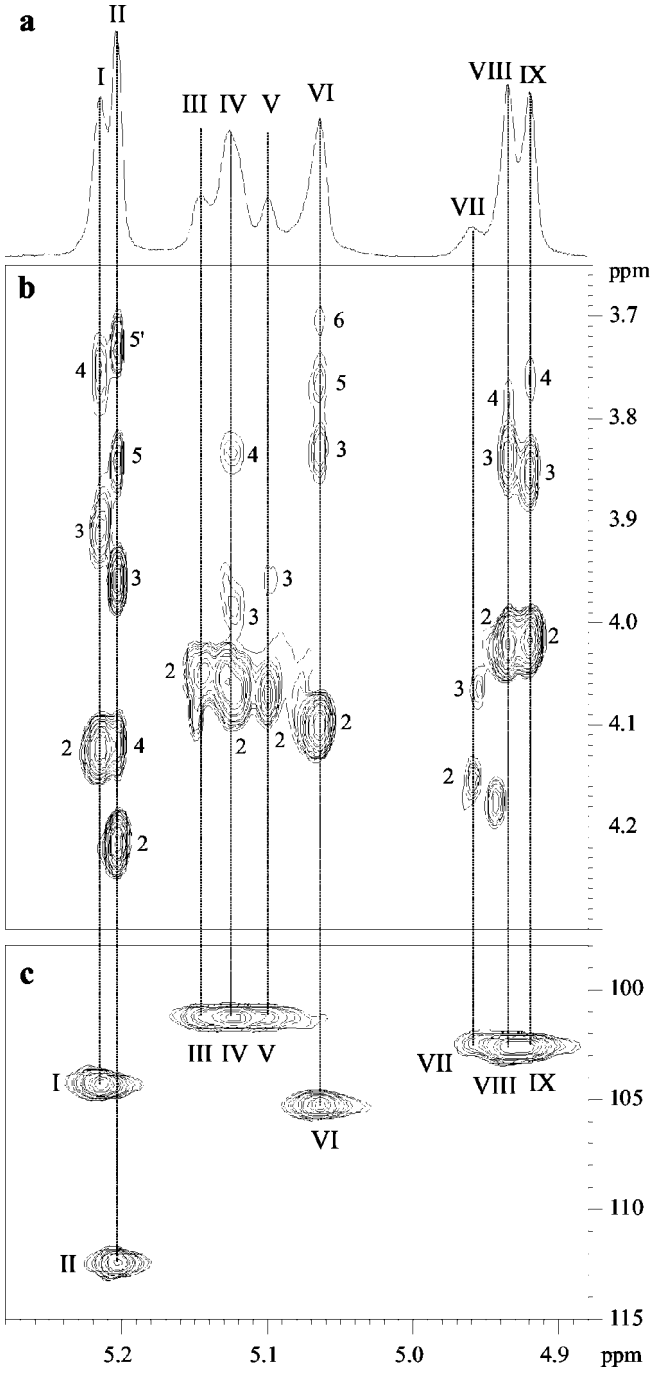

FIG. 5. **Expanded regions of the one-dimensional ^{1}H spectrum (δ^1H, 4.85–5.30) (*a*), of the two-dimensional 82-ms ^{1}H-^{1}H HOHAHA spectrum (δ^1H, 4.85–5.30 and 3.60–4.30) (*b*), and of two-dimensional ^{1}H-^{13}C HMQC spectrum (δ^1H, 4.85–5.30 and δ ^{13}C, 95–115) (*c*) in D_2O at 313 K of the ReqLAM, strain 28$^+$.** *I*, 2-α-Man*p*; *II*, t-α-Ara*f*; *III* and *IV*, 2,6-α-Man*p*; *V*, 4-α-Man*p*; *VI*, t-α-Man*p*; *VII*, *VIII*, and *IX*, 6-α-Man*p*.

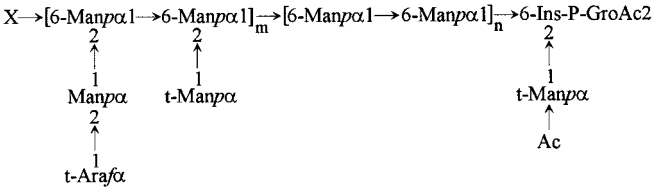

FIG. 6. **Structural model of ReqLAM.** *Ins-P-Gro-Ac$_2$*, phosphatidyl-*myo*-inositol anchor, with Ac corresponding to palmitic and tuberculostearic acids ($C_{16}/C_{t:19}$ 7/3 for 103$^+$ ReqLAM and 6/2 for 28$^+$ ReqLAM). The diacyl form represents the major acyl form. The linkage of the backbone to the *myo*-inositol anchor was postulated by analogy to the mycobacterial ManLAM anchor structure. In the same way, α-Man*p* unit was postulated in position 2 of the phosphatidyl-*myo*-inositol anchor based on the characterizations of PIM_2 which are considered as LAM precursors. NMR data indicate two domains, one corresponding to 6-*O*-linked α-Man*p* and the other to 2,6-*O*-linked α-Man*p*. From the molecular mass (8 kDa), the percentage of branching (44%) and the fact that one side chain in two was demonstrated capped with t-Ara*f*, *m* and *n* could be estimated to 6 and 8, respectively. *X* corresponds to the terminal unit, which could be assigned to either t-Ara*f* or t-Man*p*.

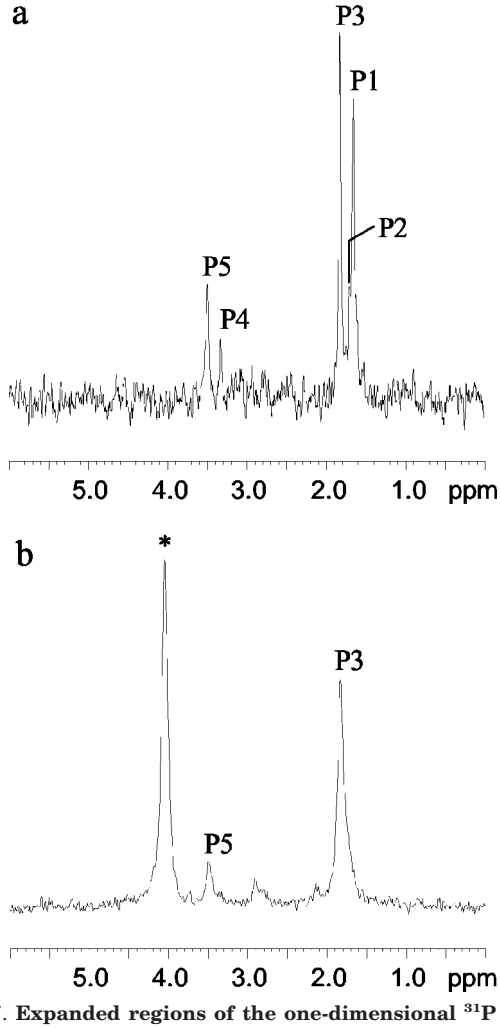

FIG. 7. **Expanded regions of the one-dimensional ^{31}P spectra (δ^{31}P, O-6) of the BCG ManLAM (*a*) and of the ReqLAM, strain 28$^+$ (*b*), in Me_2SO-d_6 at 343 K.** Signals labeled with *asterisk* correspond to non-attributed signals.

ing of 44% was estimated by the ratio of Man*p* α1→2Man*p*-APTS/Man*p*-APTS + Man*p* α1→2Man*p*-APTS. This was in agreement with the value of 46% branching obtained from alditol acetate analysis as the ratio of 2,6-*O*-linked Man*p* (27%)/2,6-*O*-linked Man*p* (27%) + 6-*O*-linked Man*p* (32%).

Purified ReqLAM from strain 28$^+$ was then analyzed by NMR. The one-dimensional ^{1}H NMR anomeric zone (Fig. 4*b*) was composed of a multitude of signals, assignment of which required more sophisticated experiments. A complete NMR strategy, involving two-dimensional ^{1}H-^{1}H COSY, HOHAHA with different mixing times, ROESY, ^{1}H-^{13}C HMQC, HMQC-HOHAHA, and HMBC, was undertaken in order to characterize the different spin systems that compose the ReqLAM (Table I) and to determine the sequence of these monosaccharidic units. This strategy was realized through NMR analysis of the

TABLE II
P_3/P_5 Gro and myo-Ins ^1H chemical shifts of strain 28^+ ReqLAM in Me_2SO-d_6 at 343 K

	myo-Ins						Gro		
	H-1	H-2	H-3	H-4	H-5	H-6	H-1/H-1′	H-2	H-3/H-3′
P-3	4.01	4.16	3.26	3.46	3.13	3.64	4.36/4.13	5.13	3.85/3.81
P-5	4.00	4.19	ND[a]	ND	3.13	3.65	4.00/ND	ND	3.79 /ND

[a] ND, not determined.

TABLE III
Oligonucleotide primer and probe sequences for amplification of various equine cytokines and the G3PDH control

Cytokine	Primer/probe	Sequence 5′–3′
G3PDH	Forward	GGTGGAGCCAAAAGGGTCAT
	Reverse	TTCACGCCCATCACAAACAT
	Probe	TCTCTGCTCCTTCTGCTGATGCCCC
IL-1β	Forward	TGAAGGGCAGCTTCCAAGAC
	Reverse	GGGAGAATTGAAGCTGGATGC
	Probe	TGGACCTCAGCTCCATGGGCGA
IL-6	Forward	CCCCTGACCCAACTGCAA
	Reverse	TGTTGTGTTCTTCAGCCACTCA
	Probe	CCTGCTGGCTAAGCTGCATTCACAGA
IL-8	Forward	CGGTGCCAGTGCATCAAG
	Reverse	TGGCCCACTCTCAATCACTCT
	Probe	CGCACTCCAAACCTTTCAATCCCAAACT
IL-10	Forward	GTCGGAGATGATCCAGTTTTACCT
	Reverse	AGTTCACGTGCTCCTTGATGTCT
	Probe	TGCCCCAGGCTGAGAACCACG
IL-12p40	Forward	TGCTGTTCACAAGCTCAAGTATGA
	Reverse	GGGTGGGTCTGGTTTGATGA
	Probe	CTACACCAGCGGCTTCTTCATCAGGG
IL-18	Forward	TGAAAACGATGAAAACCTGGAA
	Reverse	TTGGTCGTTCAAATTTCGTATGA
	Probe	CAGATTACTTTGGCAGGCTTGAACCTAAACTCTCA
IFN-γ	Forward	AAGTGAACTCATCAAAGTGATGAATGA
	Reverse	CGAAATGGATTCTGACTCCTCTTC
	Probe	TCGCCCAAAGCTAAACCTGAGGAAGC
TNF-α	Forward	GCTCCAGACGGTGCTTGTG
	Reverse	GCCGATCACCCCAAAGTG
	Probe	TGTCGCAGGAGCCACCACGCT

ManLAM[2] and ManAM (49) of the mycobacterial strain *M. bovis* BCG in D_2O and ManLAM of BCG (13) and *M. tuberculosis* (14) in Me_2SO-d_6.

The different anomeric protons were characterized by ^1H-^1H HOHAHA (Fig. 5*b*) and ^1H-^{13}C HMQC experiments, evidencing 9 spin systems, noted as I to IX in Table I. The anomeric area of the ^1H-^{13}C HMQC spectrum (Fig. 5*c*) highlights 5 anomeric C/H pairs: 104.2/5.21 (I_1); 112.3/5.20 (II_1); t 101.3 with protons at 5.15 (III_1), 5.12 (IV_1), and 5.10 (V_1); 105.2/5.06 (VI_1); 102.4/4.96 (VII_1); and 102.6 with protons at 4.93 ($VIII_1$) and 4.92 (IX_1).

The spin system II was unambiguously assigned to t-α-Ara*f*. The α anomeric configuration was based on the C-1 chemical shifts ($\delta_{C\text{-}1}$ Ara*f*, α:109.2/β:103.1). This spin system could be defined up to H-5/C-5. The different chemical shifts proved that this unit was terminal. The furanose ring was deduced from the C-4 chemical shift (δ 86.7) and from the intense cross-peak observed on the ^1H-^{13}C HMBC spectrum between the H-1 (δ 5.20) and C-4 (δ 86.7) and between C-1 (δ 112.3) and H-4 (δ 4.12) (not shown). The spin systems I, III, and IV typified 2-*O*-linked α-Man*p*. Indeed, the C-2s were found at 80.4 for system I and at 81.7 ppm for system III and IV on the two-dimensional ^1H-^{13}C HMQC-HOHAHA spectrum (not shown). The pyranose ring of system I was confirmed by the cross-peak observed on the ^1H-^{13}C HMBC between the H-1 (δ 5.21) and C-5 (δ 76.3). Concerning systems III and IV, their ^{13}C resonances were identical, highlighting a glycosylated C-6 (δ 69.9). They were assigned to 2,6-*O*-linked α-Man*p*. The chemical shifts of systems III and IV were found very similar to the ones described for the 2,6-*O*-linked α-Man*p* of the mycobacterial arabinomannan (49). System V had approximately the same anomeric chemical shifts (δ C-1 at 101.3 and δ H-1 at 5.10) as systems III and IV (Table I) and was then attributed to α-Man*p*. However, the C-2 was not found around 82 ppm on the two-dimensional ^1H-^{13}C HMQC-HOHAHA spectrum but at 73.2 ppm showing that this spin system is not C-2 glycosylated. This chemical shift was similar to the one of the C-2 of system VI (δ 73.1) which was attributed to terminal α-Man*p* (t-α-Man*p*). Spin system V was then tentatively attributed to the 4-*O*-linked α-Man*p* observed by the permethylation analysis. Then, systems VII, VIII, and IX were found to correspond to 6-*O*-linked α-Man*p* by analogy to the mycobacterial LAM.[2] Glycosylation in position C-6 was proved by the C-6 chemical shift (δ 68.7).

The glycosylated carbons were defined from the ^{13}C chemical shifts. The next step was to determine the sequence of units from ^1H-^1H ROESY and ^1H-^{13}C HMBC experiments (data not shown). The saccharidic linear core was determined to consist of 6-*O*-linked α-Man*p*. The same types of correlations were observed concerning systems VII, VIII, and IX on one side and systems III and IV on the other side: correlations between H-1 and H-6/6′ on the ^1H-^1H ROESY spectrum and between H-1 and C-6 on the ^1H-^{13}C HMBC spectrum. These correlations proved independent domains of 6-*O*-linked Man*p* and 2,6-*O*-linked Man*p*. t-Man*p* (VI) and 2-*O*-linked Man*p* (I) were observed in position 2 of the 2,6-*O*-linked Man*p* (IV) from correlations between H-1(VI)/H-2(IV) and H-1(I)/H-2(IV) on the ROESY spectrum and between H-1(VI)/C-2(IV), C-1(VI)/H-2(IV) and H-1(I)/C-2(IV), C-1(I)/H-2(IV) on the HMBC spectrum. Position 2 of 2-*O*-linked Man*p* (I) was then shown to be glycosylated by t-α-Ara*f* (II) by correlations between H-1(II)/C-2(I) on the HMBC spectrum.

In summary, the alditol acetate, permethylation, NMR, and CE data taken together allow us to propose the three following structural features for the polysaccharidic backbone (Fig. 6): (i) a domain composed of a linear chain of 6-*O*-linked α-Man*p*; (ii) linear 6-*O*-linked-α-D-Man*p* chains with side chains located at the C-2 composed of a α-Man*p* unit; and (iii) linear 6-*O*-linked-α-D-Man*p* chains with side chains located at C-2 composed of a t-Ara*f*α1→2Man*p* unit. Indeed, t-α-Ara*f* was evidenced by NMR as only capping the 2-*O*-linked α-Man*p* in agreement with the permethylation data showing that the percentage of 2-*O*-linked Man*p* (12.3%) was similar to the percentage of t-Ara*f* (10.5%). Moreover, the ratios Ara-APTS/Man*p*α1→2Man-APTS measured by CE (20:35) or (2-*O*-linked Man*p*/t-Man*p* + 2-*O*-linked Man*p*) (12.3:12.6 + 12.3) allowed us to deduce that one side chain in two was capped with t-α-Ara*f*. Moreover, the alditol acetate and permethylation data are consistent with the same structure being present in the ReqLAM from *R equi* strain 103.

Phosphatidyl-myo-inositol Anchor Acylation State—The phosphatidyl-*myo*-inositol anchor structure was investigated from one- and two-dimensional phosphorus NMR. The one-dimensional ^{31}P spectrum of ReqLAM exhibited broad unresolved signals in D_2O (not shown) consistent with multiacylated ReqLAM. Indeed, the one-dimensional ^1H NMR spectrum (Fig. 4*a*) evidenced the presence of fatty acids by the signals at 0.88 and 1.30 ppm. This was consistent with the presence of fatty acids as analyzed by GLC. The predominant fatty acids found were hexadecanoic acid (56%) and 10-methyloctadecanoic acid (tuberculostearic acid) (19%), whereas heneicosanoate, octadecenoic acid, heptadecanoic acid (C17), and a C16-

[2] M. Gilleron, T. Brando, and G. Puzo, unpublished results.

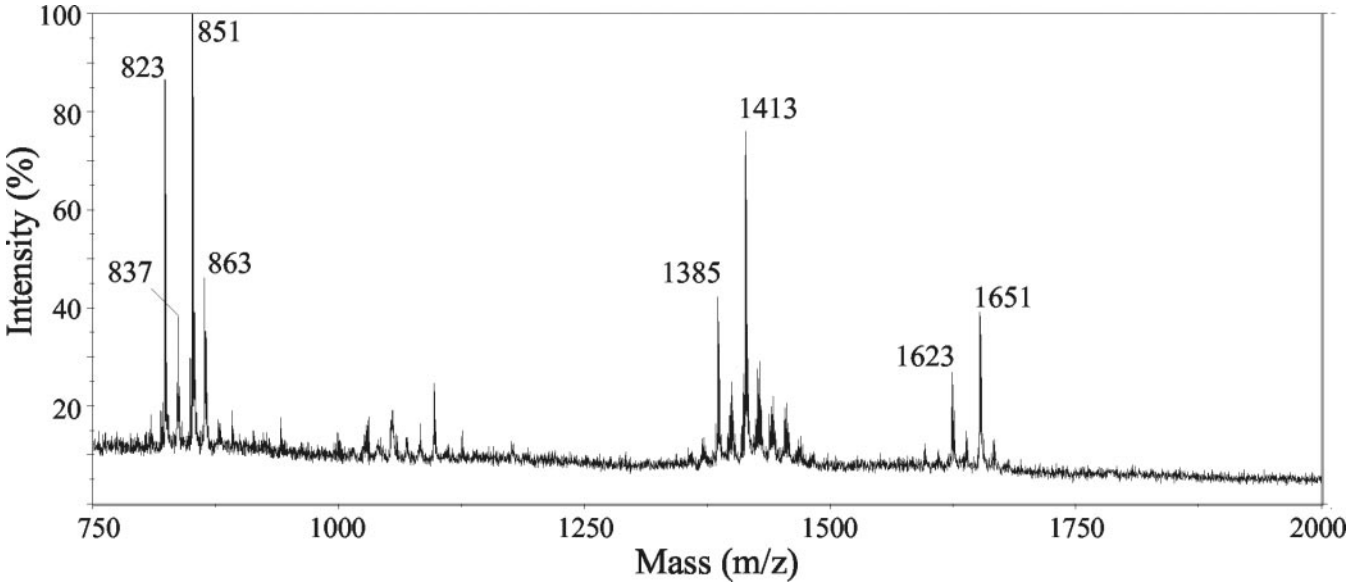

FIG. 8. **Negative MALDI-mass spectrum of the lipid extract of *R. equi* strain 28$^+$.** The peaks correspond to Ac_2PI acylated predominantly by C_{16}/C_{17} (*823*), C_{16}/C_{18} (*837*), C_{16}/C_{19} (*851*), and C_{17}/C_{19} (*863*), Ac_3PIM_2 acylated predominantly by $2C_{16}/C_{17}$ (*1385*), $2C_{16}/C_{19}$ (*1413*), and Ac_4PIM_2 acylated predominantly by $3C_{16}$, C_{17} (*1623*), and $3C_{16}$,C_{19} (*1651*).

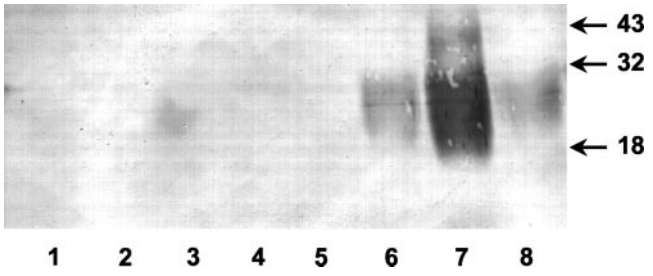

FIG. 9. **Interaction of ReqLAM with recombinant mannose-binding protein.** ReqLAM from strain 103$^+$ was loaded onto a commercial immobilized mannose-binding protein column and washed with binding buffer. Material retained by the mannose-binding protein was subsequently eluted with the manufacturer's elution buffer. Fractions were analyzed by SDS-PAGE followed by lectin blotting with concanavalin A. *Lanes 1–4*, fractions 1–4 eluted with wash buffer; *lanes 5–8*, fractions 1–4 from elution with elution buffer. The positions of the protein molecular mass standards (kDa) are marked at the *right-hand side.*

branched fatty acid (possibly 10-methylhexadecanoic acid) are present in smaller amounts (11, 6, 4, and 5%, respectively). The fatty acid composition of the lipoglycan reflected that of the whole bacterial cells (data not shown) although a reduction in the relative proportion of unsaturated fatty acids was noted, as has been observed previously (22, 25, 26) for other LAM-like lipoglycans of the mycolata.

As ReqLAM exhibited broad unresolved signals in D_2O, no connectivities between phosphate and protons could be obtained by two-dimensional ^{1}H-^{31}P HMQC and HMQC-HOHAHA. Recently, it was shown that Me_2SO-d_6 is a suitable solvent for recording high resolution one-dimensional ^{31}P NMR spectra of multiacylated mycobacterial ManLAM (13). One-dimensional ^{31}P spectrum of ReqLAM dissolved in Me_2SO-d_6 mainly showed three signals at δ 1.83, δ 3.50, and δ 4.05. From their chemical shifts and by comparison with those of the ^{31}P signals observed in the one-dimensional ^{31}P spectrum of the *M. bovis* BCG cellular ManLAM (13) (Fig. 7), two of these signals were tentatively assigned to P3 (δ 1.83) and P5 (δ 3.50).

The ^{31}P resonance assignments were confirmed with help of two-dimensional ^{1}H-^{31}P NMR spectroscopy. The ^{1}H-^{31}P HMQC-HOHAHA spectrum of ReqLAM (not shown) exhibited a complex panel of correlations. P3 showed correlations with downfield resonances at δ 5.13 in F_2 dimension, which were assigned to methine protons H-2 of di-acylated glycerol according to previous results (11, 13, 14). A similar downfield correlation was not observed for P5; instead the Gro H-2 resonance is superimposed with the Gro H-3/H-3′, indicating lack of acylation of O-2 in this minor species. So, only P3 corresponds to 1,2-di-acyl-3-phospho-*sn*-glycerol unit, and P5 corresponds to 1-acyl-2-lyso-3-phospho-*sn*-glycerol unit. The inspection of the different cross-peaks (chemical shifts, multiplicity of the signals, and $^3J_{HH}$ coupling constants), by comparison with the ^{1}H-^{31}P HMQC-HOHAHA of *M. bovis* BCG cellular ManLAM (11, 13, 14), allowed their attribution to the different protons of glycerol and *myo*-inositol spin systems (Table II). From these data, it can be proposed that P3 typified a di-acylated Gro anchor. Although the P5 signal was weak, we were able to deduce the absence of an acyl residue on C-2 of the Gro. P3 and P5 corresponded to phosphatidyl-*myo*-inositol anchor devoid of fatty acid on their *myo*-Ins unit.

The linkage of the backbone to the *myo*-inositol anchor was postulated by analogy to the mycobacterial ManLAM anchor structure. In the same way, α-Man*p* unit was postulated in position 2 of the phosphatidyl-*myo*-inositol anchor based on the characterization of PIM_2 by MALDI (Fig. 8) as PIM_2 are considered as LAM precursors.

Biological Activities of the Lipoglycan

ReqLAM showed a strong reaction on Western blotting with Hypermune-RE, an anti-*R. equi* antiserum produced commercially for the prophylactic treatment of foals (data not shown), confirming the antigenicity of the lipoglycan *in vivo*. Moreover, ReqLAM gave reactions of varying intensity with four out of four convalescent sera from foals that had recovered from *R. equi* infection (data not shown). Mycobacterial LAM, LM, and PIM have been shown to interact with MBP (50, 51). ReqLAM was applied to a column of immobilized MBP, and retention of lipoglycan material was monitored by electrophoresis followed by blotting and probing with concanavalin A (23). ReqLAM was retained by the MBP (Fig. 9), eluting only after the application of buffer containing EDTA to disrupt calcium-dependent interactions between the lipoglycan and the MBP carbohydrate recognition domain.

Further study of the biological activities of the ReqLAM

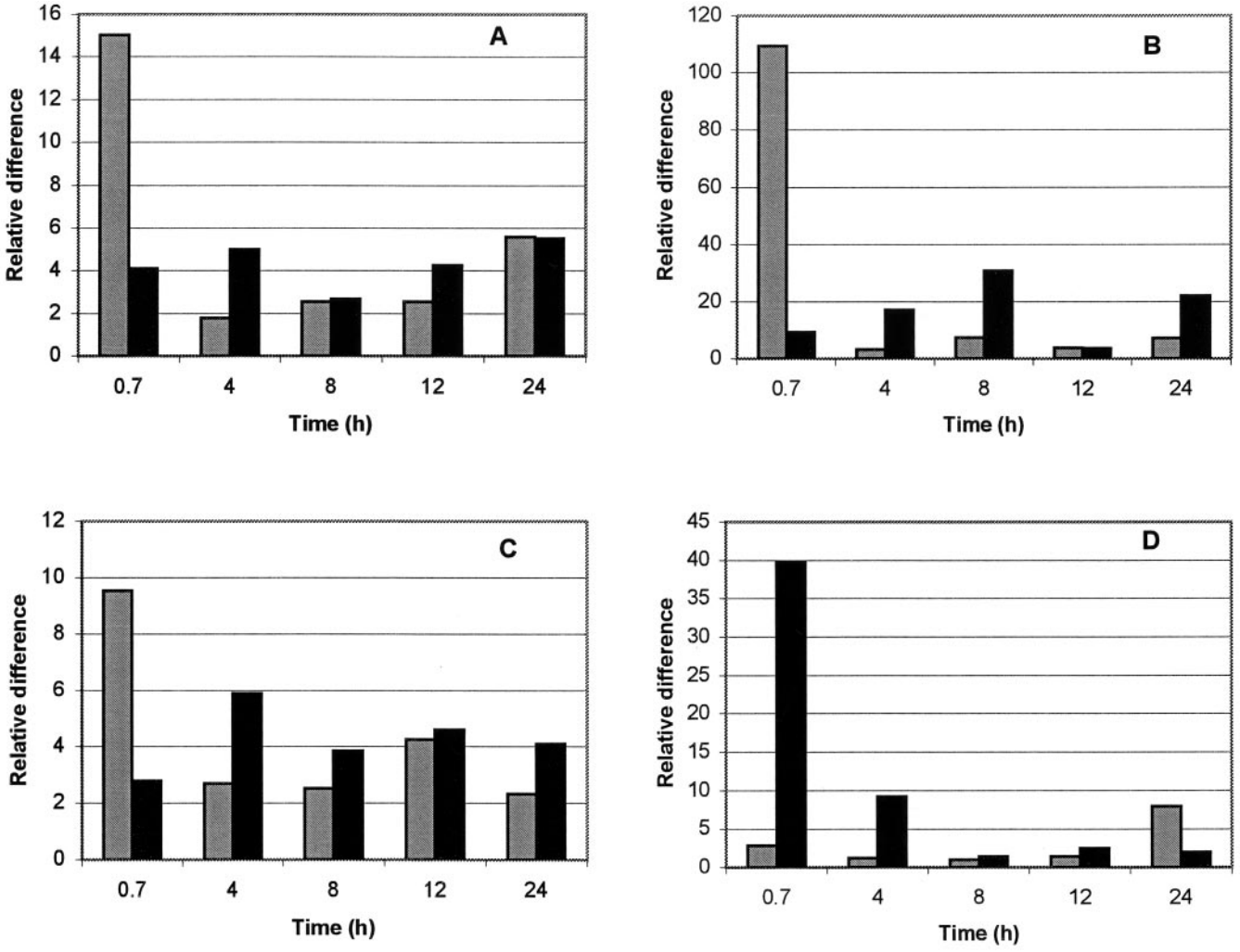

FIG. 10. **Inflammatory cytokine mRNA expression in equine macrophages infected with *R. equi* or stimulated with ReqLAM.** Equine macrophages were infected with virulent *R. equi* (*solid bars*) or incubated with 5 μg/ml of ReqLAM from strain 28^+ (*striped bars*). The induction of IL-1β (*A*), IL-6 (*B*), IL-8 (*C*), and TNF-α (*D*) mRNA expression was quantitated by real time PCR. Results are reported as the *n*-fold difference relative to cytokine mRNA expression in unstimulated macrophages.

focused on its ability to stimulate cytokine production by equine peripheral blood macrophages. Cytokines selected for study were representative of the major cytokines produced by macrophages and indicative of the development of different T cell responses. In preliminary experiments, various concentrations (1, 5, 10, or 20 μg/ml) of ReqLAM were used to stimulate equine macrophages, and TNF-α and IL-12 p40 mRNA expression was quantitated. For both cytokines, ReqLAM at 5 μg/ml induced the highest level of mRNA expression (data not shown), and therefore this concentration was used in subsequent experiments. Treatment of 5 μg/ml ReqLAM with 200 and 1,000 μg/ml polymyxin showed no inhibitory effect at either concentration on TNF-α and IL-12 p40 mRNA cytokine production over that caused by polymyxin alone (data not shown). This confirmed that ReqLAM was not contaminated by endotoxin.

Subsequently we examined cytokine induction in horse macrophages by virulent *R. equi* or by ReqLAM (5 μg/ml), at various time points. Quantitative expression of cytokine mRNA at different times following infection or lipoglycan stimulation are shown in Figs. 10 and 11. For all the representative inflammatory cytokines assayed, with the exception of TNF-α, ReqLAM induced a greater early response than the whole cells (Fig. 10) but that at later time points the overall profile of cytokine induction was similar for both *R. equi* and ReqLAM, albeit with typically higher response to the *R. equi* whole cells. Likewise, for the representative regulatory cytokines assayed, ReqLAM again induced a greater early response compared with the whole cells (Fig. 11). At later time points in the assay of the regulatory cytokines, the whole cells typically induced a greater response than the ReqLAM, with the exception of IL-18 that was not induced by either stimulant (Fig. 11*B*). The ability of ReqLAM to induce production of both inflammatory and regulatory cytokines was also confirmed in preliminary experiments with ReqLAM from strain 103+ (data not shown).

DISCUSSION

The *R. equi* lipoglycan ReqLAM has a structure related to, but clearly distinct from, that of mycobacterial ManLAM from BCG and *M. tuberculosis* (7). ReqLAM is smaller than ManLAM; MALDI-TOF mass spectrometry revealed the molecular mass of ReqLAM to be centered around 8 kDa. By using a similar method, Venisse *et al.* (15) measured the average size of ManLAM of *M. bovis* BCG as 17.4 kDa and that of LM as 6 kDa.[2] The broad diffuse band observed by SDS-PAGE and the spread of molecular mass revealed by mass spectrometry indicate that like ManLAM, ReqLAM is heterogeneous in size.

The small size of ReqLAM as compared with ManLAM is consistent with the reduced arabinose content, ~11% of the carbohydrate moiety compared with 55% for BCG ManLAM (15). The α1–6 mannan backbones of ManLAM of *M. tubercu-*

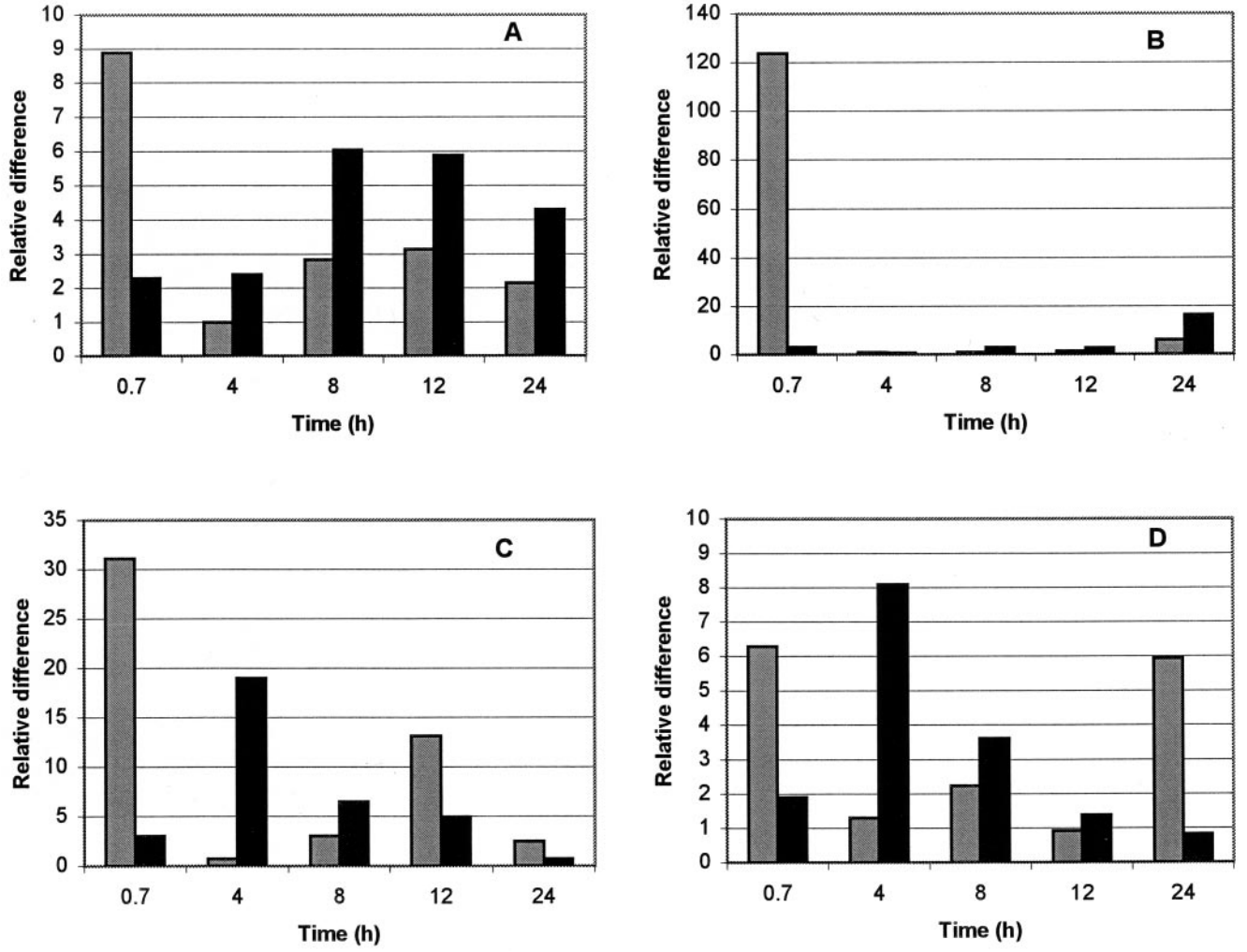

FIG. 11. **Regulatory cytokine mRNA expression in equine macrophages infected with *R. equi* or stimulated with ReqLAM.** Equine macrophages were infected with virulent *R. equi* (*solid bars*) or incubated with 5 μg/ml of ReqLAM from strain 28^+ (*striped bars*). The induction of IL-10 (*A*), IL-18 (*B*), IFN-γ (*C*), and IL-12p40 (*D*) mRNA expression was quantitated by real time PCR. Results are reported as the *n*-fold difference relative to cytokine mRNA expression in unstimulated macrophages.

losis Erdman and *M. bovis* BCG were demonstrated to be highly branched although the degree of branching and the size were heterogeneous (52, 53). Results of permethylation and CE analysis indicate that ReqLAM has a similar α1–6 mannan backbone, with ~44% of branching. Acetolysis and study of derivatized products by CE revealed the branches to contain one 2-*O*-linked mannose residue either as t-α-Man*p* or capped by t-α-Ara*f*. The majority of the arabinose residues was detected by permethylation analysis as t-α Ara*f* in agreement with the absence of mannose caps that typify the BCG and *M. tuberculosis* ManLAM (12). A structural model of ReqLAM can be proposed here, consisting of a similar mannan backbone to that of ManLAM but in which single arabinose residues decorate the mannan backbone instead of elaborate arabinan branches (Fig. 6). In agreement with its molecular mass of 8 instead of 17 kDa for the ManLAM, the arabinan domain of the ReqLAM is restricted to single α-Ara*f* capping the 2-*O*-linked α-D-Man*p*. This structural feature reveals that the biosynthesis of an extensive arabinan domain comparable with that of mycobacterial ManLAM (by addition of 5-*O*-linked α-Ara*f*) does not occur in *R. equi*, probably due to the absence of a 5-arabinosyltransferase. The reduced arabinose content of the ReqLAM may explain the relatively weak or negative cross-reactions of the lipoglycan with a polyclonal anti-LAM antiserum as the arabinose residues appear to be the principal antigenic determinants in ManLAM (7, 54). However the ReqLAM does elicit antibody production in foals and adult horses, as judged by its reaction with hyperimmune and convalescent antisera.

The presence of terminal mannose units within the ReqLAM structure (Fig. 7) may have considerable relevance with respect to the biological significance of this lipoglycan, notably through interaction with components of the innate immune response. The interaction of ReqLAM with recombinant MBP (Fig. 9) is consistent with the previously observed interaction of MBP with a variety of mannoconjugates including mycobacterial ManLAM, LM, and PIM (51) and the lipomannan of *Micrococcus luteus* (55). Binding of MBP by ReqLAM *in vivo* may activate complement C3b deposition onto *R. equi* via the lectin pathway (56) thereby helping promote the previously described (3) complement-receptor Mac-1-mediated uptake of *R. equi* into macrophages. ReqLAM may be able to bind other collectins as both LM and ManLAM have been identified as ligands for human pulmonary surfactant protein A (57), and human pulmonary surfactant protein D binds ManLAM (58), although only binding of the former surfactant promotes binding of *M. tuberculosis* to phagocytes. Equine pulmonary surfactant protein A binds mannose (59), and equine pulmonary surfactant protein D has been shown to bind both mannose and phosphatidylinositol (60). Thus ReqLAM may bind either or

both of these surfactants in the foal lung. LAM may also influence mycobacterial uptake into host cells by interacting with other receptors including macrophage mannose receptors (8, 17–19), and similar interactions may be possible for ReqLAM. Entry via some pathways, notably macrophage mannose receptors (20), may influence intracellular survival by circumventing the activation of macrophage antimicrobial responses. Consequently, the multifaceted potential of ReqLAM for promoting bacterial entry into host cells warrants further investigation.

We show here that the pro-inflammatory and immune cytokine response of equine macrophages to ReqLAM largely parallels the response to infection with live virulent *R. equi*. Activation of resident macrophages is one of the earliest responses to microbial invasion, with macrophage-derived cytokines playing a critical role in initiating the inflammatory response as well as in regulating the immune response. The results shown here suggest that much of the early macrophage cytokine response occurring after infection with *R. equi* can be attributed in part to its ReqLAM component. The effect of ReqLAM observed herein was not the result of contamination with lipopolysaccharide, because the effect could not be inhibited by use of polymyxin, which inactivates lipopolysaccharide. These findings extend and complement the results of earlier studies with infected murine macrophages, which failed to demonstrate any cytokine response that could be specifically attributed to possession of the virulence plasmid (46).

The ManLAM of *M. tuberculosis* has been shown to produce a wide spectrum of immunomodulatory functions *in vitro*, but the biological implications of these effects are still largely undefined. These effects include suppression of T-cell proliferation, inhibition of interferon (IFN)-γ-induced functions including microbicidal activity, scavenging of cytotoxic free oxygen radicals, and complement activation (7, 8, 61). However, only LAM lacking mannose caps (PILAM and AraLAM) has been found to induce significant TNF-α and IL-12 expression by human and murine macrophages (7, 8). Our studies with ReqLAM also show the marked effect of this lipoglycan on macrophage cytokine induction. It is intriguing that ReqLAM induces both pro-inflammatory cytokines (Fig. 10) and macrophage deactivating cytokines (Fig. 11). The lack of immediate TNF-α response to ReqLAM was a notable difference from the immediate TNF-α response to whole cells of *R equi* (Fig. 10*D*). Darrah and co-workers (62) have shown that both TNF-α and IFN-γ are required to activate macrophages in order to kill *R equi* by peroxynitrite. Finally, the observation of a marked optimal dose effect of ReqLAM on selected cytokine mRNA transcription (data not shown) was unexpected. Further study is needed to support the intriguing possibility that ReqLAM could produce an immunosuppressive effect through an intracellular bacterial load effect on macrophage cytokine expression. Possible effects attributable to ReqLAM thus need to be considered in future studies of the cytokine responses of equine macrophages to infection with virulent and avirulent *R. equi*.

Acknowledgments—We are grateful to Tom Barr (Veterinary Immunogenics Ltd.) for supplying the hyperimmune RE antiserum and to John Belisle (Department of Microbiology, Colorado State University) for supplying *M. tuberculosis* strain Erdman ManLAM and anti-LAM antibody (provision supported by National Institutes of Health Grant N01-AI-25147).

REFERENCES

1. Prescott, J. F. (1991) *Clin. Microbiol. Rev.* **4,** 20–34
2. Mosser, D. M., and Hondalus, M. K. (1996) *Trends Microbiol.* **4,** 29–33
3. Hondalus, M. K., Diamond, M. S., Rosenthal, L. A., Springer, T. A., and Mosser, D. M. (1993) *Infect. Immun.* **61,** 2919–2929
4. Chun, J., Kong, S.-O., Hah, Y. C., and Goodfellow, M. (1996) *J. Ind. Microbiol.* **16,** 1–9
5. Brennan, P. J., and Nikaido, H. (1995) *Annu. Rev. Biochem.* **64,** 29–63
6. Daffé, M., and Draper, P. (1998) *Adv. Microb. Physiol.* **39,** 131–203
7. Chatterjee, D., and Khoo, K.-H. (1998) *Glycobiology* **8,** 113–120
8. Strohmeier, G. R., and Fenton, M. J. (1999) *Microbes Infect.* **1,** 709–717
9. Chatterjee, D., Lowell, K., Rivoire, B., McNeil, M. R., and Brennan, P. J. (1992) *J. Biol. Chem.* **267,** 6234–6239
10. Delmas, C., Gilleron, M., Brando, T., Vercellone, A., Gheorghiu, M., Rivière, M., and Puzo, G. (1997) *Glycobiology* **7,** 811–817
11. Gilleron, M., Nigou, J., Cahuzac, B., and Puzo, G. (1999) *J. Mol. Biol.* **285,** 2147–2160
12. Monsarrat, B., Brando, T., Condouret, P., Nigou, J., and Puzo, G. (1999) *Glycobiology* **9,** 335–342
13. Nigou, J., Gilleron, M., and Puzo, G. (1999) *Biochem. J.* **337,** 453–460
14. Gilleron, M., Bala, L., Brando, T., Vercellone, A., and Puzo, G. (2000) *J. Biol. Chem.* **275,** 677–684
15. Venisse, A., Berjeaud, J.-M., Chaurand, P., Gilleron, M., and Puzo, G. (1993) *J. Biol. Chem.* **268,** 12401–12411
16. Gilleron, M., Himoudi, N., Adam, O., Constant, P., Venisse, A., Rivière, M., and Puzo, G. (1997) *J. Biol. Chem.* **272,** 117–124
17. Schlesinger, L. S., Hull, S. R., and Kaufman, T. M. (1994) *J. Immunol.* **152,** 4070–4079
18. Venisse, A., Fournié, J.-J., and Puzo, G. (1995) *Eur. J. Biochem.* **231,** 440–447
19. Schlesinger, L. S., Kaufman, T. M., Iyer, S., Hull, S. R., and Marchiando, L. K. (1996) *J. Immunol.* **157,** 4568–4575
20. Astarie-Dequeker, C., N′Diaye, E-N., Le Cabec, V., Rittig, M. G., Prandi, J., and Maridonneau-Parini, I. (1999) *Infect. Immun.* **67,** 469–477
21. Dahl, K. E., Shiratsuchi, H., Hamilton, B. D., Ellner, J. J., and Toossi, Z. (1996) *Infect. Immun.* **64,** 399–405
22. Sutcliffe, I. C. (1995) *Arch. Oral Biol.* **40,** 1119–1124
23. Sutcliffe, I. C. (2000) *Antonie Leeuwenhoek* **78,** 195–201
24. Ikeda-Fujita, T., Kotani, S., Tsujimoto, M., Ogawa, T., Takahashi, I., Takada, H., Nagao, S., Kokeguchi, S., Kato, K., Yano, I., Okamura, H., Tamura, T., Harada, K., Usami, H., Yamamoto, A., Tanaka, S., and Kato, Y. (1987) *Microbiol. Immunol.* **31,** 289–311
25. Flaherty, C., and Sutcliffe, I. C. (1999) *Syst. Appl. Microbiol.* **22,** 530–533
26. Flaherty, C., Minnikin, D. E., and Sutcliffe, I. C. (1996) *Zbl. Bakteriol.* **285,** 11–19
27. Takai, S. (1997) *Vet. Microbiol.* **56,** 167–176
28. Chatterjee, D., Hunter, S. W., McNeil, M. R., and Brennan, P. J. (1992) *J. Biol. Chem.* **267,** 6228–6233
29. Assaf, N. A., and Dick, W. A. (1993) *BioTechniques* **15,** 1010–1015
30. Sutcliffe, I. C. (1994) *Syst. Appl. Microbiol.* **17,** 321–326
31. Leopold, K., and Fischer, W. (1993) *Anal. Biochem.* **208,** 57–64
32. Fox, J. D., and Robyt, J. F. (1991) *Anal. Biochem.* **195,** 93–96
33. Laemmli, U. K. (1970) *Nature* **227,** 680–685
34. Tsai, C. M., and Frasch, C. E. (1982) *Anal. Biochem.* **119,** 115–119
35. Beachey, E. H., Dale, J. B., Simpson, W. A., Evans, J. D., Knox, K. W., Ofek, I., and Wicken, A. J. (1979) *Infect. Immun.* **23,** 618–625
36. Dell, A., Reason, A. J., Khoo, K.-H., Panico, M., McDowell, R. A., and Morris, H. R. (1994) *Methods Enzymol.* **230,** 108–132
37. Saddler, G. S., Tavecchia, P., Lociuro, S., Zanol, M., Colombo, L., and Silva, E. (1991) *J. Microbiol. Methods* **14,** 185–191
38. Nigou, J., Vercellone, A., and Puzo, G. (2000) *J. Mol. Biol.* **299,** 1353–1362
39. Guttman, A., Chen, F. T., Evangelista, R. A., and Cooke, N. (1996) *Anal. Biochem.* **233,** 234–242
40. Marion, D., and Wuthrich, K. (1983) *Biochem. Biophys. Res. Commun.* **113,** 967–974
41. Bax, A., and Davis, D. G. (1985) *J. Magn. Res.* **65,** 355–360
42. Bax, A., and Subramanian, S. (1986) *J. Magn. Res.* **67,** 565–569
43. Shaka, A. J., Barker, P. B., and Freeman, R. (1985) *J. Magn. Res.* **64,** 547–552
44. Lerner, L., and Bax, A. (1986) *J. Magn. Res.* **69,** 375–380
45. Bax, A., and Summers, M. F. (1986) *J. Am. Chem. Soc.* **108,** 2093–2094
46. Giguère, S., and Prescott, J. F. (1998) *Infect. Immun.* **66,** 1848–1854
47. Leutenegger, C. M., Mislin, C. N., Sigrist, B., Ehrengruber, M. U., Hofmann-Lehmann, R., and Lutz, H. (1999) *Vet. Immunol. Immunopathol.* **71,** 291–305
48. Nigou, J., Gilleron, M., Cahuzac, B., Bounéry, J.-D., Herold, M., Thurnher, M., and Puzo, G. (1997) *J. Biol. Chem.* **272,** 23094–23103
49. Nigou, J., Gilleron, M., Brando, T., Vercellone, A., and Puzo, G. (1999) *Glycoconj. J.* **16,** 257–264
50. Hoppe, H. C., de Wet, B. J. M., Cywes, C., Daffé, M., and Ehlers, M. R. W. (1997) *Infect. Immun.* **65,** 3896–3905
51. Polotsky, V. Y., Belisle, J. T., Mikusova, K., Ezekowitz, R. A. B., and Joiner, K. A. (1997) *J. Infect. Dis.* **175,** 1159–1168
52. Chatterjee, D., Khoo, K.-H., McNeil, M. R., Dell, A., Morris, H. R., and Brennan, P. J. (1993) *Glycobiology* **3,** 497–506
53. Venisse, A., Rivière, M., Vercauteren, J., and Puzo, G. (1995) *J. Biol. Chem.* **270,** 15012–15021
54. Gaylord, H., Brennan, P. J., Young, D. B., and Buchanan, T. M. (1987) *Infect. Immun.* **55,** 2860–2863
55. Polotsky, V. Y., Fischer, W., Ezekowitz, R. A. B., and Joiner, K. A. (1996) *Infect. Immun.* **64,** 380–383
56. Matsushita, M. (1996) *Microbiol. Immunol.* **40,** 887–893
57. Sidobre, S., Nigou, J., Puzo, G., and Rivière, M. (2000) *J. Biol. Chem.* **275,** 2415–2422
58. Ferguson, J. S., Voelker, D. R., McCormack, F. X., and Schlesinger, L. S. (1999) *J. Immunol.* **163,** 312–321
59. Hobo, S., Ogasawara, Y., Kuroki, Y., Akino, T., and Yoshihara, T. (1999) *Am. J. Vet. Res.* **60,** 169–173
60. Hobo, S., Ogasawara, Y., Kuroki, Y., Akino, T., and Yoshihara, T. (1999) *Am. J. Vet. Res.* **60,** 368–372
61. Hetland, G., Wiker, H. G., Hogasen, K., Hamasur, B., Svenson, S. B., and Harboe, M. (1998) *Clin. Diagn. Lab. Immunol.* **5,** 211–218
62. Darrah, P. A., Hondalus, M. K., Chen, Q., Ischiropoulos, H., and Mosser, D. M. (2000) *Infect. Immun.* **68,** 3587–3593

A Novel Lipoarabinomannan from the Equine Pathogen*Rhodococcus equi* : STRUCTURE AND EFFECT ON MACROPHAGE CYTOKINE PRODUCTION

Natalie J. Garton, Martine Gilleron, Thérèse Brando, Han-Hong Dan, Steeve Giguère, Germain Puzo, John F. Prescott and Iain C. Sutcliffe

J. Biol. Chem. 2002, 277:31722-31733.
doi: 10.1074/jbc.M203008200 originally published online June 18, 2002
